



# Mechanical performance of integrally bonded copper coatings for the long term disposal of used nuclear fuel



Christopher H. Boyle<sup>a,\*</sup>, Shaker A. Meguid<sup>b</sup>

<sup>a</sup> Nuclear Waste Management Organization, 22 St. Clair Ave East, Toronto, Canada

<sup>b</sup> Department of Mechanical and Industrial Engineering, University of Toronto, 5 King's College Road, Toronto, Canada

## HIGHLIGHTS

- A novel Used Fuel Container with an integrally bonded copper coating is proposed.
- Two developed coating processes successfully produced prototype container components.
- We created a validated finite element model to predict coating structural performance.
- Mechanical testing confirms coating suitability for repository use.

## ARTICLE INFO

### Article history:

Received 15 April 2015

Received in revised form 29 June 2015

Accepted 4 August 2015

## ABSTRACT

The preferred method for disposal of used nuclear fuel is underground emplacement in a Deep Geological Repository (DGR). Many countries have light water reactor fuels which require large Used Fuel Container or Canister (UFC) designs weighing up to 25 ton for containment. In contrast, Canada exclusively uses heavy water reactor fuel, which is substantially smaller. This has led the Nuclear Waste Management Organization (NWMO) to create a novel UFC, which uses standard pressure vessel grade steel for structural containment and a thick, integrally bonded copper coating applied to the exterior surface for corrosion protection. Currently, the coating is applied using two different methods: electrodeposition and gas dynamic cold spray. This novel copper coating needs to be fully validated to ensure adequate mechanical strength and chemical resistance for use under repository conditions. Detailed mechanical and corrosion testing programs were undertaken. Mechanical tests indicated that adhesion strengths exceeded 45 MPa and tensile properties were comparable to wrought copper. A Finite Element Model (FEM) of the copper–steel composite was created and validated using three point bend tests. This model accurately predicts the response of the composite, including large deformation and debonding failure mechanisms. Now validated, this model will be used to assess the performance of the coating on the full-scale UFC under simulated DGR loading conditions.

© 2015 The Authors. Published by Elsevier B.V. This is an open access article under the CC BY-NC-ND license (<http://creativecommons.org/licenses/by-nc-nd/4.0/>).

## 1. Introduction

The internationally preferred method for the long-term disposal of used nuclear fuel is a *Deep Geological Repository* (DGR). Many countries, including Sweden, Switzerland, and Canada, began DGR research and development as early as the 1970s. Currently, there are several additional countries pursuing DGRs, including Finland, Japan, Korea, Belgium, France, and the United Kingdom. The long-term safety of a DGR relies on the use of multiple *engineered barrier systems* (EBS), which provide redundant containment, isolation,

and retardation functions, as shown in Fig. 1. The EBS consists of used or spent fuel bundles packaged into a long-lived *Used Fuel Container* or *Canister* (UFC). The container is surrounded by bentonite clay, which retards the flow of water and suppresses microbial growth (Wolfaardt and Korber, 2012; Stroes-Gascoyne et al., 2010). The DGR is constructed at a depth of over 400 m. The geosphere of dense rock, which has no free flowing water, limits the movement of radioactive particles. Natural analogues of DGRs, such as the Cigar Lake uranium deposit, have effectively isolated high-grade uranium ore for millions of years (Miller et al., 1994).

Since the beginning of DGR research and development in the 1970s, copper has been a favored material for container corrosion prevention. Copper was selected due to its thermodynamic stability from corrosion under DGR conditions and several natural analogues

\* Corresponding author. Tel.: +1 6472593736.  
E-mail address: [cboyle@nwmo.ca](mailto:cboyle@nwmo.ca) (C.H. Boyle).

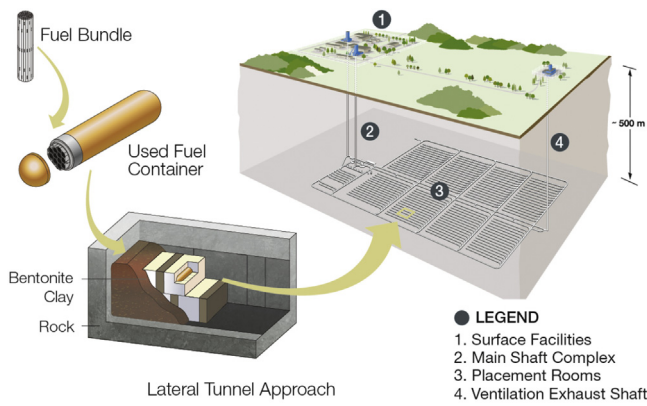


Fig. 1. Canada's Deep Geological Repository (DGR) concept.

proving its performance. These analogues include archaeological artifacts (King, 1995) (i.e. coins, cannons, etc.), which contain metallic copper, as well as, mineral deposits that contain naturally occurring metallic copper (Chastain et al., 2011). In addition, corrosion processes that impact the lifespan of copper within a DGR have been extensively studied for over 30 years by the international community. Most recent efforts by Canada's Nuclear Waste Management Organization (NWMO) (Kwong, 2011), as well as independent corrosion experts (Scully and Edwards, 2013) have focused on developing and reviewing corrosion allowances to account for all the processes that significantly affect copper materials. From these reviews, a copper corrosion allowance of less than 1.3 mm has been deemed appropriate for one million years storage in a Canadian DGR. This corrosion allowance is very conservative; it is expected that much less than 1.3 mm of copper will corrode over that time period.

Sweden and Finland have proposed a "dual-vessel" container design consisting of a large cast-iron inner vessel for structural strength with a 50 mm thick copper overpack vessel for corrosion protection. This concept is known as the KBS-3 (Svensk Kärnbränslehantering AB, 2010). NWMO also has a reference dual-vessel container design; however, a key design difference is the use of a hollow inner steel shell for the containment vessel instead of a honeycomb cast-iron insert. Canada's heavy water CANDU reactors use small, natural uranium fuel bundles, which can be packaged as densely as possible with negligible risk of criticality in water or air. As a result, a shell design allows more efficient storage of CANDU bundles by the use of internal baskets. While the dual-vessel design is technically feasible, there are several potential challenges for implementation. From a functional perspective, a nominal radial gap of less than 2 mm between the inner and outer vessel has been identified as a requirement to limit the creep strain (Raiko et al., 2010) and prevent rupture from low creep ductility (Pettersson, 2012). This requires manufacturing a 9 to 14 t steel or cast-iron vessel and a 7.5 t copper vessel almost 5 m in length with tight radial fit-up tolerances, followed by precision assembly. The assembled UFC is then handled from the copper vessel and needs to support the entire ~25 t loaded container weight. Consequently, the thickness of the copper shell must be much greater than what is required for corrosion protection.

Adaptive phased management (APM) is the NWMO's technical method and management system for implementing Canada's DGR (NWMO, 2005). APM emphasizes adaptability and incorporation of evolving knowledge and technology. This philosophy has driven an initiative to develop an alternative UFC for Canada's unique CANDU fuel and geosphere, which overcomes some of the potential issues inherent to the dual-vessel design. This UFC, known as the Mark II and shown in Fig. 2, is under development with several novel design concepts:

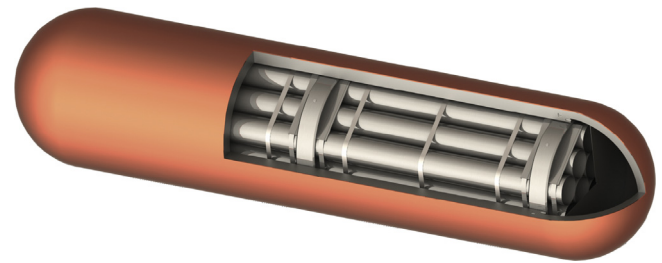


Fig. 2. NWMO's Mark II Used Fuel Container for CANDU bundles (cut-away shown for clarity). Approximate dimensions 562 mm (~22") diameter, 2514 mm (~99") length.

- **Copper coating:** is integrally supported by the steel structural substrate. The thickness is driven by the corrosion allowance requirement and can be tailored to site-specific requirements.
- **Hemi-spherical heads:** better distribution of the external pressure load resulting in biaxial compressive stresses. Flat head designs can produce the tensile stresses due to bending; tension is undesirable in the container as it is a key component in crack growth mechanisms, such as, Stress Corrosion Cracking (SCC) and fatigue.
- **Pressure vessel materials:** The proposed design uses common, weld understood nuclear pressure vessel grade materials and sizes. For example, the shell is manufactured from standard sized extruded steel pipe or small forgings, approved for use by ASME Section 3 for storage containments. A benefit of using these materials is ease of availability (compared to large sized custom casting or forgings).
- **Manageable size:** Many international nuclear waste management organizations have very large steel or cast iron UFCs, weighing up to 25 t once loaded. Handling and underground emplacement of such heavy containers requires large, custom equipment. The size of these containers is driven by the light water reactor fuel, which can exceed 4 m in length. In contrast, Canada's CANDU fuel is only a half metre in length. This allowed the NWMO to optimize the UFC dimensions for this smaller fuel type. The resulting Mark II UFC weighs less than 3 t and could potentially be handled using radiation shielded conventional sized forklift trucks.

The most novel aspect of this container is the copper coating. This concept allows for direct deposition of the copper corrosion barrier layer onto the steel or cast-iron structural components, forming a robust metallurgical or mechanical bond resulting in a single, unified UFC composite structure. Assembly tolerances and creep rupture issues are resolved. Additionally, the thickness of the copper can be tailored to the site specific geosphere and environment. Currently, NWMO is proposing a 3 mm copper layer based on the previously stated corrosion requirement; however, various thicknesses up to 10 mm are being investigated within ongoing work programs.

The objective of this work is to develop a robust, copper coating which can be applied to disposal containers for the safe disposal of used nuclear fuel in a DGR. To accomplish this, two novel copper coating processes were studied: gas dynamic cold spray and pulsed electrodeposition. During process development, coating quality was measured against two major functional requirements: corrosion and mechanical performance. Chemically, the copper coating must have equivalent or exceed the corrosion performance of the reference wrought copper that is currently proposed. This work is ongoing and preliminary results have been published elsewhere (Jakupi, 2015; Keech et al., 2014). Mechanically, the copper coating must have sufficient strength, ductility, and adhesion to withstand all loadings under DGR conditions. An experimentally validated mechanical integrity model of the copper coating was developed to predict its behaviour under beyond design basis loading, including

potential failure mechanisms. This model will be used to evaluate the performance of the coatings as applied to the Mark II UFC design under repository loading conditions.

This paper will present an overview of the coating processes and product characterization, the novel mechanical integrity model used to predict the mechanical performance of the coating, and the experimental testing used to validate this model.

## 2. Methods

### 2.1. Coating process development

The coating process development had three main objectives:

1. The performance of the copper coating, both the mechanical structural response and chemical corrosion resistance, must meet or exceed that of the wrought copper as determined by experimental testing.
2. The coating process must ensure that repeatable, fully dense coatings are produced.
3. The coating process is feasible for large scale container manufacturing.

The NWMO has investigated several different coating methods including: weld overlay, gas dynamic cold spray, and electrodeposition. Cold spray and electrodeposition processes facilitate the production of high purity coatings (i.e., no alloy additions); on this basis, these methods were selected for further development described herein. The test program incorporated the application of coatings to steel substrates used in Mark II UFC fabrication, including plate, pipe, and hemi-sphere product forms, ranging in thickness from 12 to 46 mm. Both coating methods are described in detail elsewhere (Papyrin et al., 2006; Aust et al., 2008).

Gas dynamic cold spray or “cold spray” involves the acceleration of powders within an inert carrier gas to high velocities, at which they impact a substrate and form a strong mechanical bond (Irissou et al., 2008). The method is similar to thermal spray coatings but the temperature of the powder does not exceed the melting temperature - a solid state process. As a result, the deposited layer has identical chemical properties as the initial powder feed. While very high deposition rates can be obtained by a single gun (i.e. up to 1 kg/min), it has been primarily used as a repair process within industry. Within the NWMO program, both low pressure cold spray (LPCS) and high pressure cold spray (HPCS) have been investigated, for complete UFC coverage (i.e. factory supplied components), partial UFC coverage (i.e. coating weld closure zone after final assembly), and coating repair. The use of cold spray for UFC manufacture is also being investigated by the Korean nuclear waste management program (Choi et al., 2010).

Electrodeposition involves immersion of two electrodes into a specialized chemical bath solution. A current is applied to the electrodes, oxidizing the anode material producing dissolved cations in the solution, which are then reductively plated at the cathode. For this application, a high purity, oxygen free copper anode was used as the copper source and pressure vessel grade steel was the substrate cathode. Pyrophosphate was used as the primary bath solution to minimize carbon and oxygen content within the copper coating and pulsed potentiometry was used to apply sufficient current. In this application, electrodeposition would be used to supply pre-coated UFC components.

### 2.2. Coating mechanical performance

The primary function of the copper coating is a corrosion barrier. Nonetheless, to remain an effective barrier it must be fully dense

and have adequate strength and ductility to remain adhered to the container under DGR loadings. Mechanical failure of the coating in the DGR would result in exposure of the more reactive steel substrate to groundwater and potentially compromise containment. To ensure adequate mechanical performance the following testing was performed for several copper coatings: as deposited cold spray, annealed cold spray (two variations, 1 h@350°C and 600°C), and as deposited electrodeposition.

Tensile tests were performed according to ASTM E08-04 (ASTM, 2008a) to generate stress–strain curves, as shown in Fig. 3. Five specimens of each material were prepared by wire electric discharge machining. The yield strength, ultimate tensile strength, and overall strain were calculated from the curves. In addition to the coatings, the ASTM A516 Gr.70 (ASTM, 2010) carbon steel substrate was also tested in the as-received and annealed conditions.

Adhesion strength tests were performed to measure the bond strength of the bimetallic copper–steel interface. ASTM C633-01 (ASTM, 2008b) is the standard testing method for adhesion strength of thermal/cold spray coatings. The testing methodology involves applying the coating to a 1” diameter plug manufactured from the substrate material, which is bonded to a separate blank plug using a strong adhesive bonding agent (such as epoxy). For this work, the selected bonding agent required a curing heat treatment of ~150°C for 1 h.

A limitation of ASTM C633-01 testing standard is the use of a bonding agent. Commercial high strength adhesives provide bond strength up to 60–70 MPa before failing in the epoxy; as a result, the test may only identify that the coating adhesion exceeds this minimum epoxy strength. To determine the actual adhesion strength, a modified version of the ASTM E08-04 tensile test is used. A bimetallic copper–steel micro specimen, similar to those in the ASTM E8 tensile standard, were manufactured and tested using a custom fixture, as shown in Fig. 3. Fifteen specimens for each coating were prepared. This method allows an accurate measurement of adhesion strength, as the geometry ensures failure in the bulk copper or at the bimetallic interface.

Three point bend tests were performed to assess ductility, resistance to cracking, and debonding of the copper–steel composite. The testing and specimen geometry followed the guided U-bend test in accordance with ASTM E290-09 (ASTM, 2009). The thicknesses of the copper and steel substrate were ~3 mm and ~6.5 mm, respectively, for a total specimen thickness of ~9.5 mm (3/8” as per the standard). Five specimens were tested for each coating type. The testing apparatus measured the force–deflection response throughout the bend. The specimens were filmed with a high-resolution camera during testing to determine the onset of surface defects and debonding.

It is important to note that the three point bend test represents an extreme loading scenario, far exceeding the container deflections and strains resulting from the DGR loads. The container’s steel substrate and copper coating are designed to remain in the elastic range during normal expected loadings (i.e. groundwater hydrostatic head and bentonite swelling). Even in extreme loading scenarios, including the hydrostatic pressure from a 3000 m thick glacier positioned over the repository would induce strains less than 1% in the copper coating. The purpose of this beyond design basis test is to validate the performance of the copper coating mechanical integrity model and to ensure it can accurately predict the coating’s behaviour including potential failure mechanisms.

### 2.3. Coating mechanical integrity model

A coating mechanical integrity model, which can accurately predict the behaviour of the copper–steel composite at the bimetallic interface and in the bulk materials, is presented. The

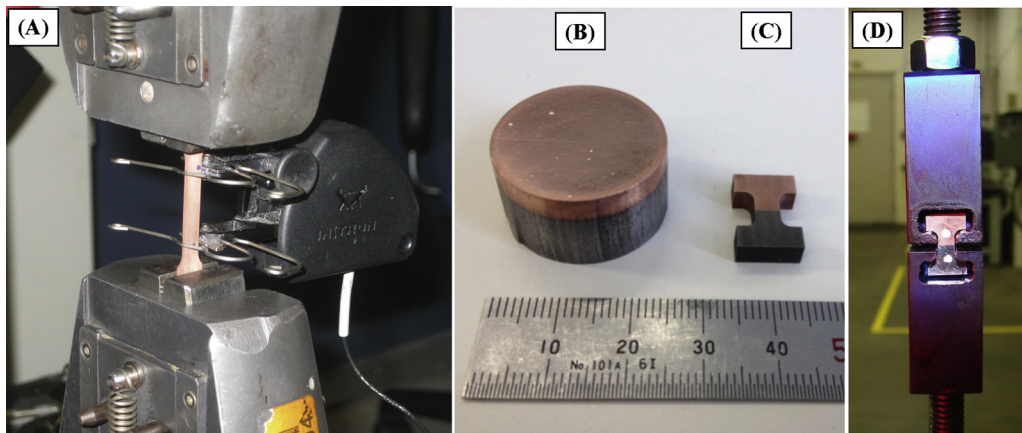


**Fig. 3.** Copper coating material property testing: (A) ASTM E08-04 tensile testing, (B) ASTM C633-01 adhesion test plug specimen, (C) modified ASTM E08-04 adhesion “Dog Bone” specimen, (D) custom test fixture for modified E08 adhesion testing.

following methodology was used to develop and validate the model:

1. *Material characterization:* The individual tensile properties of the copper coating(s) and steel substrate; as well as, the corresponding adhesion properties were experimentally determined.
2. *Development of the coating mechanical integrity model:* A Finite Element Model (FEM) of the bimetallic copper–steel composite was developed. The bimetallic interface bond is implemented using the numerical Cohesive Zone Model (CZM) for contact/interface elements. If the failure criteria are met, the CZM will initiate the fracture and debonding of the coating. The experimentally determined tensile and adhesion properties act as the inputs to the model.
3. *Experimental validation via three point bend testing:* Using the developed model, simulations of the three-point bend tests for the various copper–steel specimens were completed. The computational results, including the force–deflection response and onset of debonding, were compared to the experimental bend tests.

CZM is a numerical fracture mechanics technique, which was originally developed to predict crack growth in concrete but has since been applied to other materials and failure mechanisms (Hillerborg et al., 1976). The bilinear CZM formulation, as proposed by Alfano and Crisfield (2001), was implemented to model debonding between the copper–steel interface and crack propagation in the bulk copper coating. The expected container loads act normal to the coating surface and do not create substantial shearing loads at the bimetallic interface, therefore tangential slip will not significantly contribute to coating debonding. At this time, the tangential slip failure criteria are assumed to be identical to normal separation (i.e. failure is Mode I dominated). The bilinear CZM constitutive model employs a linear softening relationship between the normal cohesive contact stress and the interface separation distance (contact gap) to simulate the debonding process.

The finite element modeling of the three-point bend test specimens, as shown in shown in Fig. 4, was completed in ANSYS V14.5 software (ANSYS). Non-linear, large deformation formulation was used. All material properties were taken from the experiments discussed above. Isotropic strain hardening with maximum distortion energy theory flow rule was used to model the plastic deformation behaviour of both the copper coatings and steel substrate. Two CZM zones were implemented: between the bimetallic interface and in the bulk copper coating. Failure in the bulk coating theoretically occurs at the centre of the specimen due to the high tensile loads;

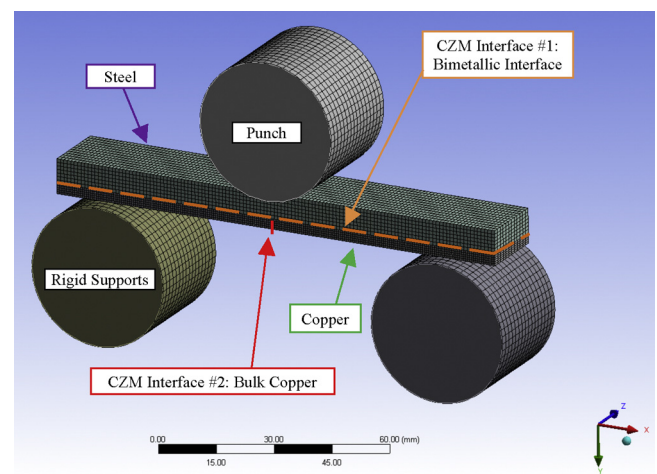


**Fig. 4.** Three-point bend specimen geometry and cohesive zone model (CZM) interface locations.

therefore, the CZM model triggers failure if the experimental ultimate tensile strength is reached (99% of the experimental tensile value is used to avoid numerical instability). The second CZM model at the bimetallic interface triggers debonding if the experimental adhesion strength is exceeded. The guided U-bend supports and punch are manufactured from high strength steel and assumed to be rigid in order to reduce computational effort. The punch is loaded incrementally to a total deflection of 30 mm, identical to the experiment, to make an approximate 90° bend in the specimen.

### 3. Results and discussion

#### 3.1. Coating process development

Gas dynamic cold spray process development commenced with characterizing high purity, low-oxygen copper powders. Fig. 5 demonstrates typical powder shape/size used in high pressure cold spray (HPCS) coatings. The next phase of development optimized various cold spray operating parameters, such as gas pressure, pre-heating, and feed rate. These were all experimentally tested for mechanical performance and the top performers selected. It was determined that cost effective coatings could be produced via two stages: initially a 50–100 μm bond coat or “strike layer” was deposited using helium as a carrier gas, followed by a bulk coating deposited using nitrogen.

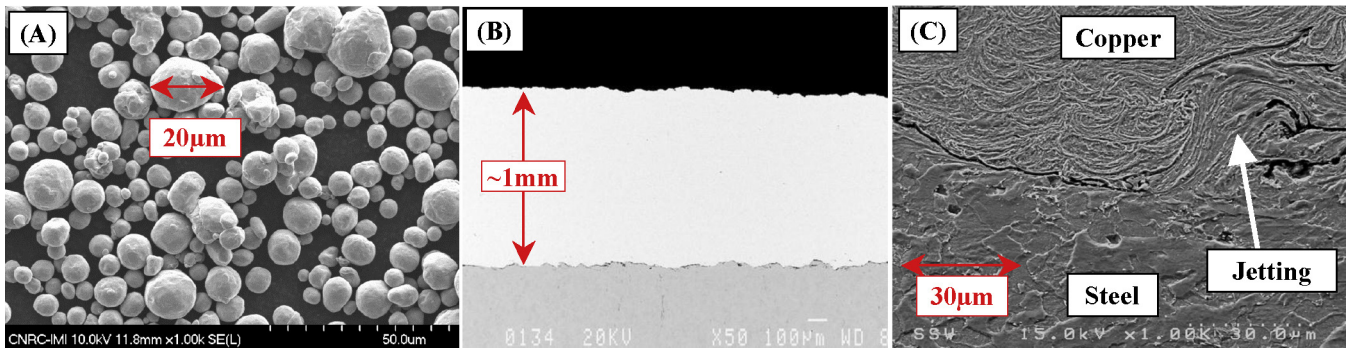


**Fig. 5.** Scanning electron microscope analysis of cold spray copper characteristics (A) low-oxygen copper powder, (B) cross-section of fully dense test coating, (C) cross-section depicting “Jetting” Bond.

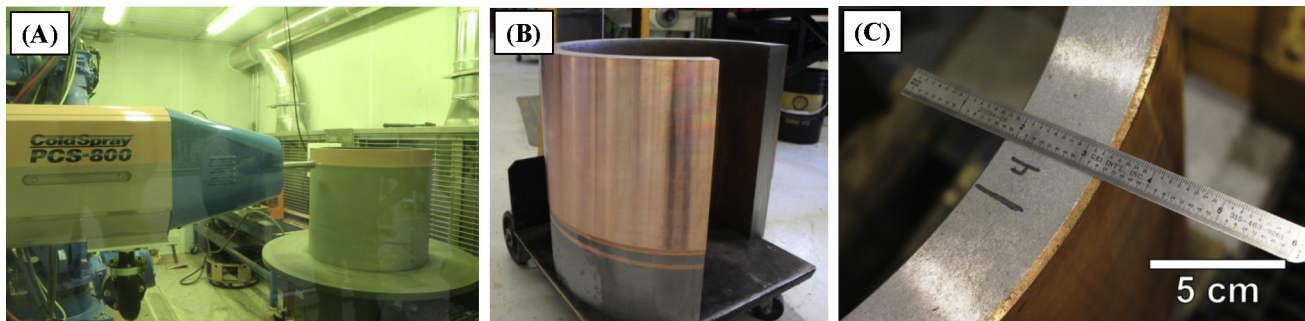


**Fig. 6.** Cold spray coating on 20” diameter pipe segment (A) cold spray equipment and process, (B) machined coating, (C) section showing >3 mm fully dense copper coating.

The constant high velocity impact of particles results in a homogeneous coating, as shown in Fig. 5, with no noticeable individual particle geometry remaining. The intimate mixing between the copper coating and steel substrate, a process known as “jetting”, is also visible. Jetting is a visual indication that the coating has good adherence onto the substrate. After coating parameter optimization, the final task was to ensure feasibility of coating actual container geometry. The technology was used to successfully coat the pressure vessel shell material to a thickness exceeding 3 mm, as shown in Fig. 6.

The deposited coating material strain hardens due to the high impact velocity and bonding process. This highly cold worked structure exhibits decreased ductility and increased yield strength. However, material properties consistent with polycrystalline wrought copper can be achieved by annealing

the as-deposited coating (Eason et al., 2012). Several different annealing temperatures are being evaluated within ongoing research.

Electrodeposition process development focused on optimizing the bath solution chemistry and the pulsed current application to ensure a uniform, fine grained, high purity deposited copper layer. The developed electrodeposited copper samples exhibited high tensile strength, ductility, and adhesion. In contrast to cold spray, no post deposition annealing is required. For this initial work deposition rates per unit area were generally slow, with the 3 mm coating taking approximately 72 h to produce. However, the nature of the process allows similar deposition rates regardless of the coating area (i.e. small plates or the container can be coated in the same time). The process is also easily scalable, making parallel production of multiple containers possible. The technology was

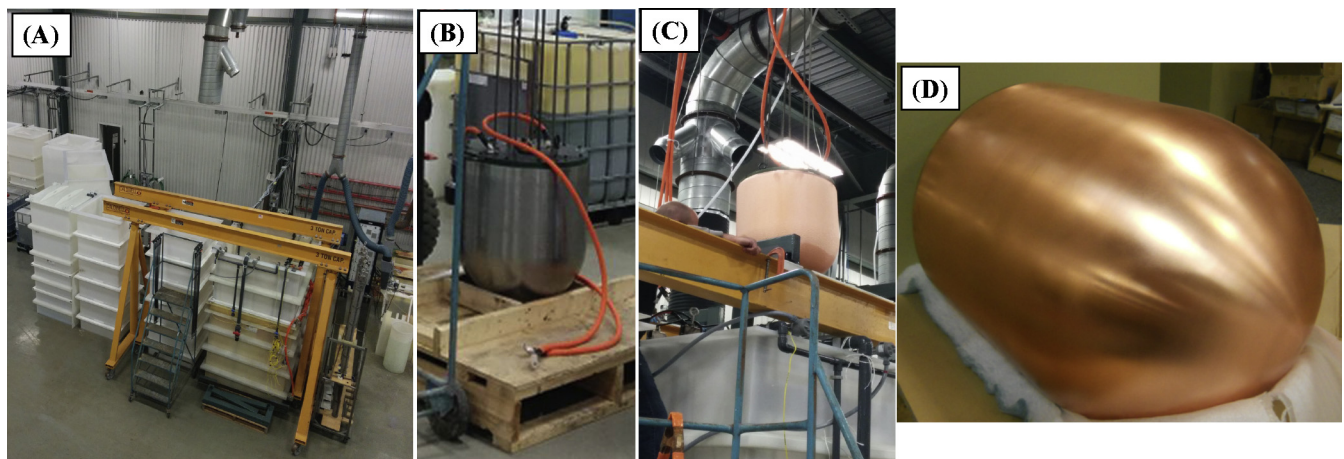


**Fig. 7.** Electrodeposited coating on 22” diameter mock-up Mark II container section (A) electrodeposition solution tanks, (B) steel mock-up prior to immersion, (C) as-deposited mock-up removed from tank, (D) machined mock-up with 3 mm thick copper coating.

**Table 1**  
Tensile strength and ductility of used fuel container materials.

Specimens	Yield strength (offset 0.2%) [MPa]	Ultimate tensile strength [MPa]	Strain [%]
A516 Gr.70—as received (normalized)	340.05 ± 7.24	511.02 ± 7.92	24.33 ± 0.19
A516 Gr.70—annealed 1 h@350 °C	338.09 ± 9.50	507.96 ± 5.20	24.61 ± 0.51
A516 Gr.70—annealed 1 h@600 °C	318.12 ± 1.37	471.53 ± 3.98	26.69 ± 0.33
Copper cold spray—as-deposited	N/A	170.55 ± 14.45	0.22 ± 0.04
Copper cold spray—annealed 1 h@350 °C	103.08 ± 2.90	198.37 ± 6.52	23.22 ± 3.04
Copper cold spray—annealed 1 h@400 °C	97.49 ± 0.90	194.05 ± 9.77	25.91 ± 5.71
Copper cold spray—annealed 1 h@600 °C*	83.56 ± 1.82	194.91 ± 9.10	27.08 ± 5.35
Copper electrodeposition—as-deposited	226.1 ± 4.7	312.1 ± 6.2	43.1 ± 5.6
Wrought SKB OFP-copper (Sandström et al., 2009)	~70	~194	~38

\* NOTE: 2 specimens failed outside the gage length and were not considered.

used to successfully coat a mock-up Mark II container section to a thickness exceeding 3 mm, as shown in Fig. 7.

### 3.2. Coating mechanical performance

Tensile properties of the various copper coatings and steel substrates, as summarized in Table 1, were comparable to or exceeded the reference SKB wrought copper with the exception of the as-deposited cold spray as expected. The ductility of the cold spray coatings varied depending on the degree of annealing. The as-deposited samples consistently had maximum strains of less than 0.3% resulting in immediate brittle fracture. As the annealing temperatures increased, ductility increased while yield strengths decreased. Large variability in maximum strain at fracture was noted for the annealed specimens with the standard deviation ranging from 13 to 22% of the mean. The variability in the 600 °C annealed specimens was compounded since two tests were excluded due to failure outside the gage length. Despite the variability, these preliminary results indicate that post-deposition annealing can achieve strengths and ductility suitable for the container.

Representative stress–strain curves of the various coatings are shown in Fig. 8. In order to demonstrate the variability of the tensile

**Table 2**  
Adhesion strength of copper coatings.

Specimens	Adhesion strength (modified ASTM E8-04) [MPa]	Experiment notes
Cold spray—as-deposited	83.3 ± 15.0	Failure in bulk copper
Cold spray—annealed 1 h@350 °C	67.0 ± 4.8	Failure in bulk copper
Cold spray—annealed 1 h@600 °C	45.9 ± 5.9	Failure in bulk copper, near steel interface
Electrodeposition—as-deposited	329.8 ± 43.6	Failure in bulk copper, necking prior to fracture

data, two curves depicting the lowest and highest achieved strains at fracture are presented for each process (with the exception of the low performance, as-deposited cold spray). The A516 Gr.70 steel substrate was also tested in the as-received (normalized) and annealed conditions. The measured yield strength exceeded the minimum 260 MPa specified by the product form standard for all conditions. The annealed specimens had slightly lower strength but increased ductility.

The adhesion strength testing results are summarized in Table 2 and typical specimen failures are shown in Fig. 9. The cold spray specimens failed in the bulk coating and exhibited no yielding

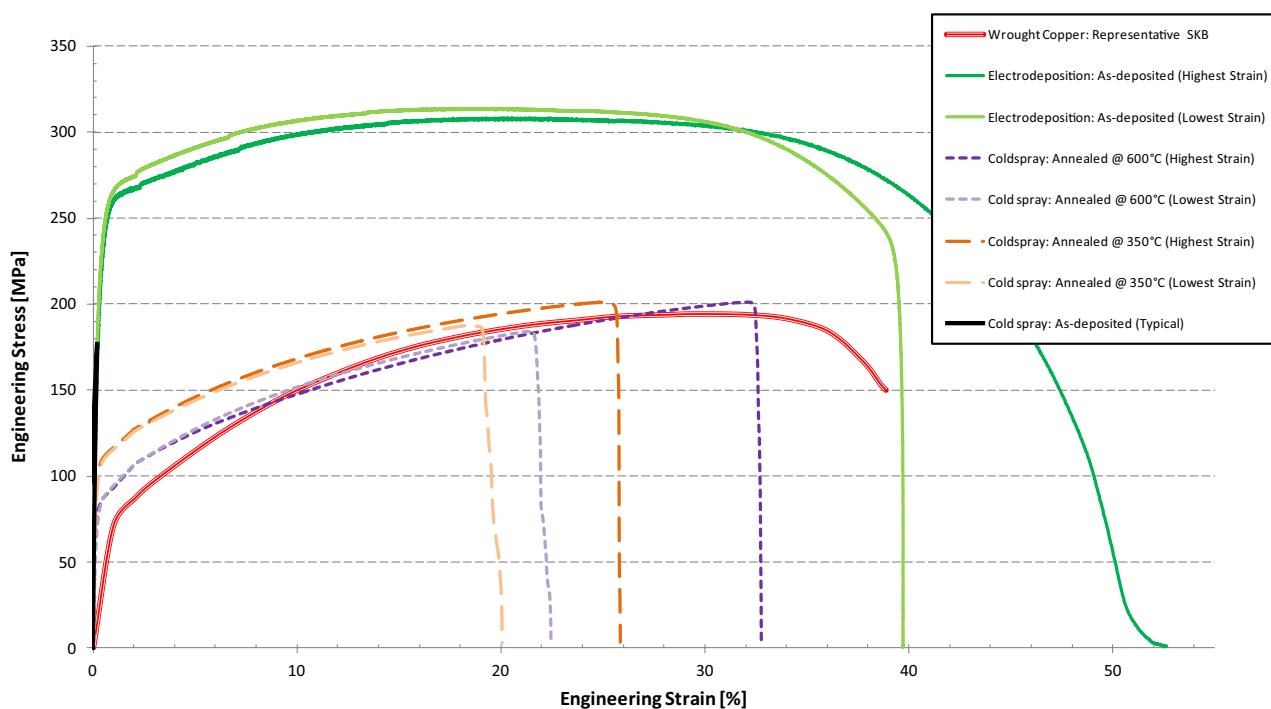


**Fig. 8.** Engineering stress–strain curves of various copper coatings versus wrought copper. The results of the coating specimens with the lowest and highest strain at fracture are shown.

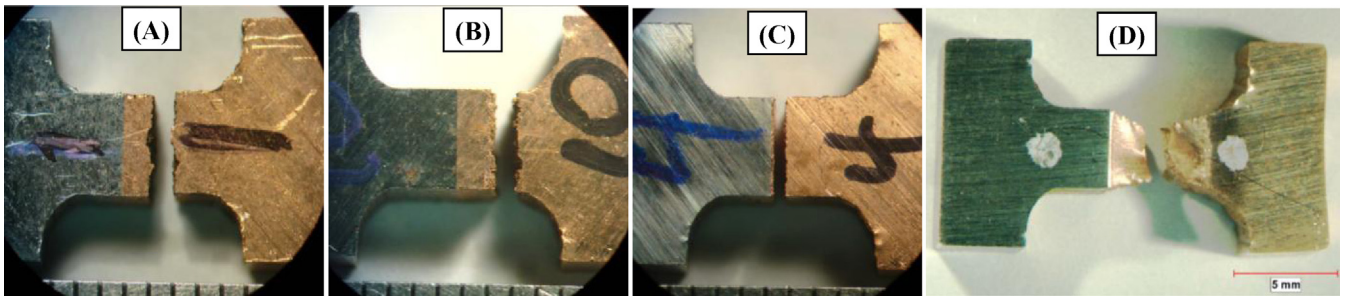


Fig. 9. Typical copper coating adhesion test results: (A) cold spray as-deposited, (B) cold spray annealed (1 h@350 °C), (C) cold spray annealed (1 h@600 °C), (D) electrodeposition as-deposited.

before failure. The electrodeposited also failed in the bulk copper; however, significant necking occurred. This demonstrates that the adhesion strength of the steel-copper interface likely exceeds the ultimate tensile strength of the bulk electrodeposited copper.

Three-point bend testing results are shown in Figs. 10–12. All as-deposited cold spray specimens exhibited surface cracks in less than a millimetre of loading. The cracks propagated quickly through the bulk coating to the substrate, followed by full debonding failure at the copper–steel bimetallic interface as observed in Fig. 10. As loading continued, the copper coating progressively peeled away from the substrate leaving no residual copper at the interface. The annealed cold spray coatings performed much better, reaching 50° to 80° bend before crack formation, correlating to ~15–28 mm of deflection. This high variability of initial failure deflection is discussed in Section 3.3. Once a crack developed it propagated rapidly and debonding ensued, similar to the as-deposited cold spray. Examination of the bimetallic interface post-failure revealed a thin residual copper layer that remained adhered to the steel substrate. This is hypothesized to be the initial helium strike layer. Fig. 11 shows the onset of crack formation for the 600 °C samples; as well as, full debonding at maximum bend. The 350 °C samples performed similarly. The electrodeposited coating demonstrated the

best performance reaching the full 90°+ bend without any cracking or debonding on all five specimens; a typical results is shown in Fig. 12.

### 3.3. Coating mechanical integrity model

The coating mechanical integrity model was compared to the experimental three-point bend tests for four coatings: as-deposited cold spray, annealed cold spray (1 h@350 °C), annealed cold spray (1 h@600 °C), and as-deposited electrodeposition using the force–deflection curves and onset of cracking. Comparison of the model and experimental force–deflection curves, as shown in Figs. 10–12, reveal good agreement. To demonstrate the influence of the tensile property inputs, two simulations were completed for each coating type, corresponding to the lowest and highest strains at fracture for the tensile data experimentally obtained.

Fig. 13 shows the good correlation between the force deflection curve for the as-deposited cold spray samples and the FEM. The peak force at initial crack formation ranged from 4857 to 5128 N occurring at 0.62–0.83 mm of deflection. For the model, peak force ranged from 4623 to 4679 N at 0.60 mm of deflection were predicted corresponding the lowest and highest tensile performance,

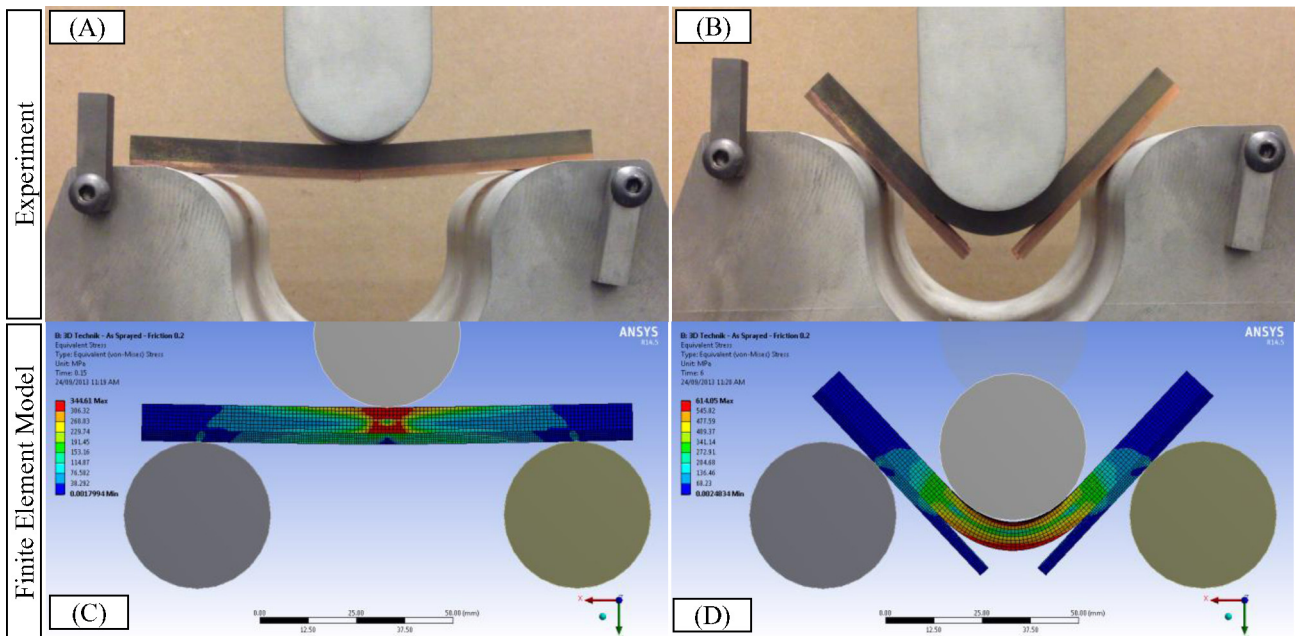


Fig. 10. Three-point bend results for as-deposited cold spray: (A and C) crack-initiation, (B and D) debonding at full-bend. (A and B) Experimental results versus (C and D) model results.

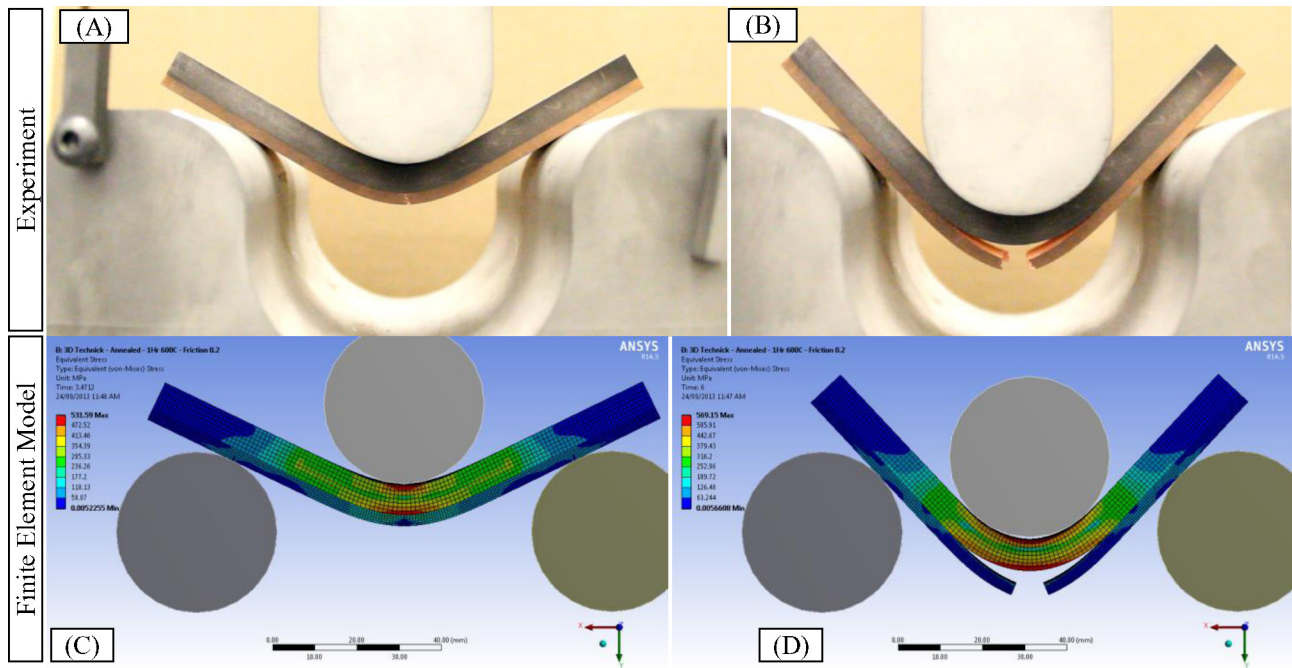


Fig. 11. Three-point bend results for 600 °C annealed cold spray: (A and C) crack-initiation, (B and D) debonding at full-bend. (A and B) Experimental results versus (C and D) model results.

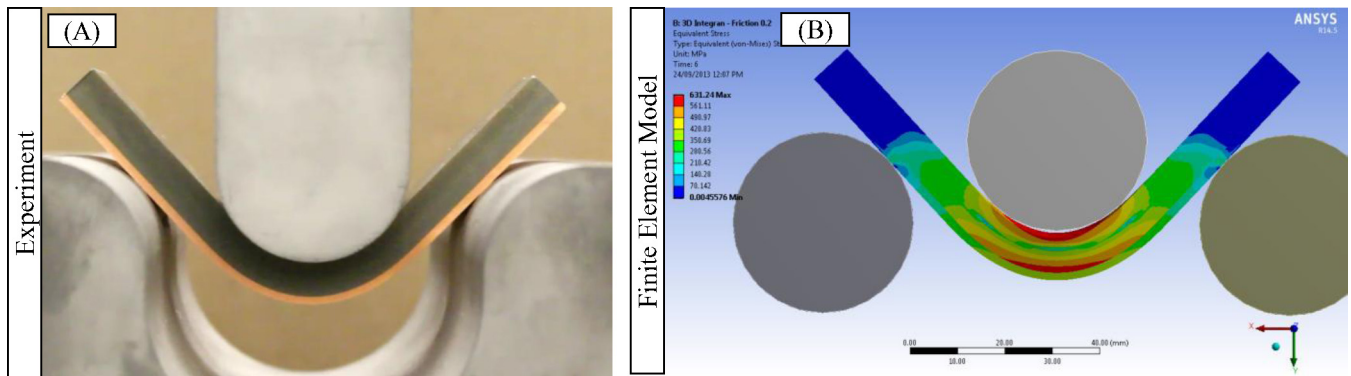


Fig. 12. Three-point bend results for as-deposited electrodeposition: no debonding at full bend (A) experimental result versus (B) model results.

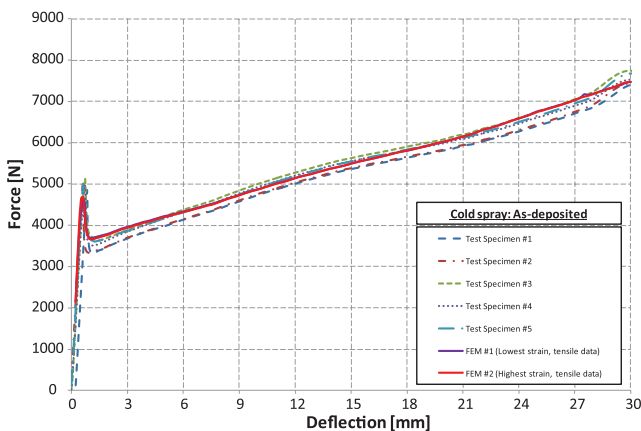


Fig. 13. Three-point bend force–deflection response: as deposited cold spray.

respectively. After debonding began, the model’s predicted force response falls within the range of experimental results, as shown in Fig. 13. At full bend, the experimental and model peak forces ranged from 7408 to 7741 N.

As previously mentioned, the annealed cold spray specimens showed the largest variability terms in performance, as reflected in Figs. 14 and 15. For the 350 °C annealed specimens, all yielded at approximately ~4500 N and 1 mm of deflection, then had a similar response up to 15 mm of deflection. Specimens then failed at 16–24 mm of deflection, with final peak forces between 8172 and 8745 N. The model predicted crack initiation at ~13.5 and 20.4 mm for lowest and highest strain tensile data, respectively.

For the 600 °C annealed specimens, all yielded at approximately ~4100 N and 1 mm of deflection, then had a similar response up to 15 mm of deflection. A total of three specimens failed between 15 and 18 mm and the final two failed at 20 mm and 27 mm, as can be observed in Fig. 15. For the four specimens that failed between 15 and 20 mm, the final peak force was 7149–7268 N. The model predicted crack initiation at ~16.5 mm for the lowest strain tensile data, followed by rapid propagation and coating debonding. The final peak force was 7156 N, which is within the range of the experimental results. For the highest strain tensile data, the model predicted no coating failure; however, the resulting peak strain is within 5% of the ultimate strain and is close to failure. It is hypothesized that inhomogeneities inherent to the cold spray process act

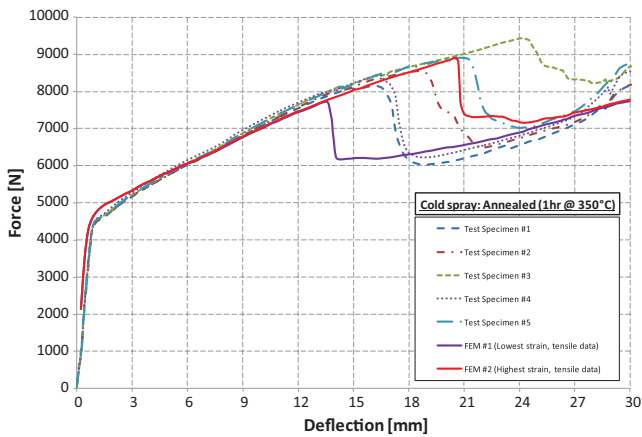


Fig. 14. Three-point bend force–deflection response: annealed (1 h@350°C) cold spray.

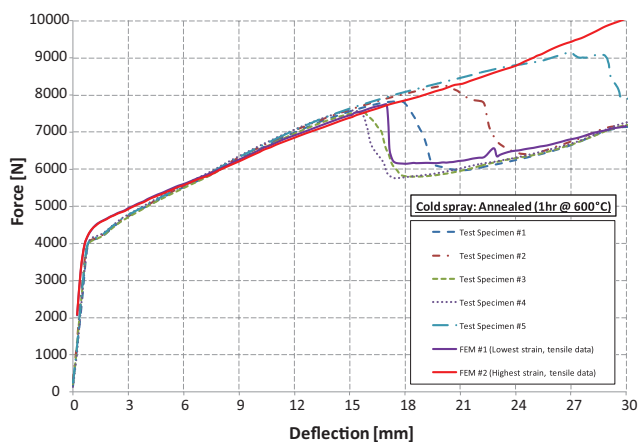


Fig. 15. Three-point bend force–deflection response: annealed (1 h@600°C) cold spray.

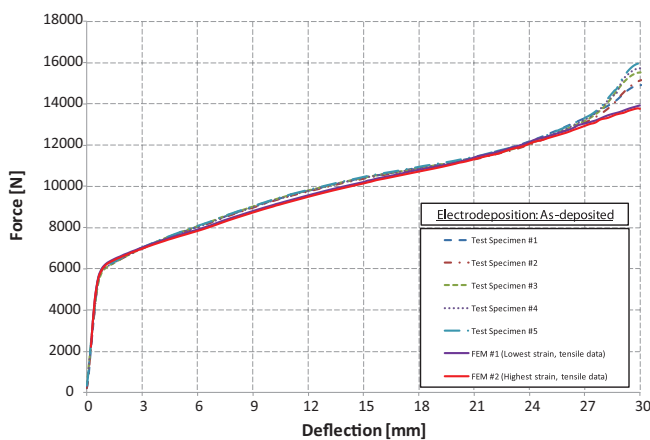


Fig. 16. Three-point bend force–deflection response: as deposited electrodeposition.

as stress risers and are enough to initiate localized failure zones not captured in the model.

For the electrodeposited specimens, yielding occurred at ~6000 N and subsequent loading produced no failures of the coating for all specimens, as shown in Fig. 16. The model also predicted no failure using both the lowest and highest strain tensile data and followed the experimental force–deflection response within 4% up to 27 mm of deflection. Although no cracking occurs, the peak

strain is within 3–11% of predicted failure. For the final 3 mm of loading, the experimental specimen's peak force increased substantially to 14,920–15,983 N; whereas, the model's near linear increase resulted in a peak force of 13,748–13,919 N. The reason for this rise is unknown.

In summary, the results confirm that the modeling can accurately predict the behaviour of the copper–steel composite including failure at the bimetallic interface. The predicted failure mechanisms, final deformed geometries, and force–deflection curves were consistent with the experimental results, as shown in Figs. 13–16. The annealed cold spray results showed high variability in the tensile testing; as a result, the three-point bend tests produced a wide range of failures. Cold spray process optimization is still ongoing and fabrication variability continues to be reduced. As previously mentioned, it is important to note that preliminary UFC design analysis has shown the copper strains would be much less than 1% even under the glacial loading scenario. Even the worst performing annealed cold spray coating test specimens exceeded 20% strain and would be at no risk of failure. The three point bend loadings represent a beyond design basis scenario with induced strains approaching 28% at full bend.

#### 4. Conclusion

The experimental development and mechanical modeling of a robust copper coating for use as a Used Fuel Container corrosion barrier has been presented. Cold spray and electrodeposition coatings with comparable mechanical performance to wrought copper have been fabricated on the full-scale container materials.

The mechanical performance of the annealed cold spray and as deposited electrodeposition coatings were comparable or exceeded that of the reference wrought copper and are suitable for the container design. Variability in the performance of cold spray coatings was noted. This work represents only the initial “proof of concept” results; as part of future work, additional process refinements and research into alternative annealing schedules will be completed to reduce this variability and improve overall performance.

A mechanical integrity model for the copper–steel composite was developed and experimentally validated. It accurately predicted the various copper coating responses, including the bimetallic interface failure. The model's average force response deviated less than 4% from the experiments, with localized maximums of approximately 10–15%. For future work, this model will be used to evaluate the performance of the coatings on the Mark II UFC under repository loading conditions; as well as, beyond design basis analyses to demonstrate the conservativeness of the design.

In conclusion, this work demonstrates that copper coatings can be reliably fabricated on container materials and geometries. These coatings have been extensively tested and confirm ample mechanical performance for container design. We can accurately model their response under expected repository conditions and beyond. Production of full-scale containers, additional optimization of coating parameters, and application of the model to container geometries are currently underway.

#### Acknowledgments

Coating process development, optimization, and experimental work has been conducted in collaboration with Integran Technologies Inc. and the National Research Council Canada facilities.

#### References

- Alfano, G., Crisfield, M.A., 2001. Finite element interface models for the debonding analysis of laminated composites: mechanical and computational issues. *Int. J. Numer. Methods Eng.* 50, 1701–1736.

- ANSYS® Mechanical, Release 14.5. Help System, Workbench. ANSYS Inc., Canonsburg, PA. <http://www.ansys.com/Industries/Academic/Tools/Citations>
- ASTM, 2008a. Standard test methods for tension testing of metallic materials. In: ASTM E8/E8M-08. ASTM International, West Conshohocken, PA.
- ASTM, 2008b. Standard test method for adhesion or cohesion strength of thermal spray coatings. In: ASTM C633-01. ASTM International, West Conshohocken, PA.
- ASTM, 2009. Standard test methods for bend testing of material for ductility. In: ASTM E290-09. ASTM International, West Conshohocken, PA.
- ASTM, 2010. Standard specification for pressure vessel plates, carbon steel, for moderate- and lower-temperature service. In: ASTM A516/516M-10. ASTM International, West Conshohocken, PA.
- Aust, K., Brooks, I., Gonzalez, F., Lin, P., Palumbo, G., Tomantschger, K., Nagarajan, N., 2008. Method for preparing polycrystalline structures having improved mechanical and physical properties. Canadian Patent No. 2674403.
- Chastain, M.L., Deymier-Black, A.C., Kelly, J.E., Brown, J.A., Dunand, D.C., 2011. Metallurgical analysis of copper artifacts from Cahokia. *J. Archit. Sci.* 38, 1727–1736.
- Choi, H.J., Lee, M., Lee, J.Y., 2010. Application of a cold spray technique to the fabrication of a copper canister for the geological disposal of CANDU spent fuels. *Nucl. Eng. Des.* 240 (10), 2714–2720.
- Eason, P.D., Kennett, S.C., Eden, T.J., Krull, I., Kowalski, B., Jones, J.L., 2012. *In situ* observation of microstrain relief in cold-sprayed bulk copper during thermal annealing. *Scr. Mater.* 67, 791–794.
- Hillerborg, A., Modeer, M., Petersson, P-E., 1976. Analysis of crack formation and crack growth in concrete by means of fracture mechanics and finite elements. *Cem. Concr. Res.* 6, 773–782.
- Irissou, E., Legoux, J.-G., Ryabinin, A., Jodoin, B., Moreau, C., 2008. Review on cold spray process and technology: Part I. Intellectual property. *J. Therm. Spray Technol.* 17, 495–516.
- Jakupi, P., Keech, P.G., Barker, I., Ramamurthy, S., Jacklin, R.L., Shoesmith, D.W., Moser, D.E., 2015. Characterization of commercially cold-sprayed and electrodeposited copper grains on mild steel. *J. Nucl. Mater.* 466, 1–11.
- Keech, P.G., Vo, P., Ramamurthy, S., Chen, J., Jacklin, R., Shoesmith, D.W., 2014. Design and development of copper coatings for long term storage of used nuclear fuel. *Corros. Eng. Sci. Technol.* 49, 425 (Special Issue on Corrosion in Nuclear Waste Systems).
- King, F., 1995. A natural analogue for the long-term corrosion of copper nuclear waste containers—reanalysis of a study of a bronze cannon. *Appl. Geochem.* 10, 477–487.
- Kwong, G.M., 2011. Status of corrosion studies for copper used fuel containers under low salinity conditions. In: NWMO Technical Report, NWMO-TR-2011-14. Nuclear Waste Management Organization, Toronto, Canada.
- Miller, W.M., Chapman, N., McKinley, I., Alexander, R., Smellie, J.A.T., 1994. *Natural Analogue Studies in the Geological Disposal of Radioactive Wastes*. Elsevier Science, Amsterdam, The Netherlands.
- NWMO, 2005. *Choosing a Way Forward: The Future Management of Canada's Used Nuclear Fuel*. Nuclear Waste Management, Toronto, Canada.
- Papyrin, A., Kosarev, V., Klinkov, S., Alkhimov, A., Fomin, V.M., 2006. *Cold Spray Technology*. Elsevier, Amsterdam, The Netherlands.
- Petterson, K., 2012. A review of the creep ductility of copper for nuclear waste canister application. In: SSM Technical Note 2012:13. Strålsäkerhetsmyndigheten, Stockholm, Sweden.
- Raiko, H., Sandström, R., Rydén, H., Johansson, M., 2010. Design analysis report for the canister. In: SKB Technical Report TR-10-28. Svensk Kärnbränslehantering AB, Stockholm, Sweden.
- Sandström, R., Hallgren, J., Burman, G., 2009. Stress Strain flow curves for Cu-OFP. In: SKB Rapport R-09-14. Svensk Kärnbränslehantering AB, Stockholm, Sweden.
- Scully, J.R., Edwards, M., 2013. Review of NWMO copper corrosion allowance. In: NWMO Technical Report, NWMO-TR-2013-04. Nuclear Waste Management Organization, Toronto, Canada.
- Stroes-Gascoyne, S., Hamon, C.J., Maak, P., Russell, S., 2010. The effects of the physical properties of highly compacted smectitic clay (bentonite) on the culturability of indigenous microorganisms. *Appl. Clay Sci.* 47, 155–162.
- Svensk Kärnbränslehantering AB, 2010. Design and production of the KBS-3 repository. In: SKB Technical Report TR-10-12. Svensk Kärnbränslehantering AB, Stockholm, Sweden (updated 2013-10).
- Wolfaardt, G.M., Korber, D.R., 2012. Near-field microbiological considerations relevant to a deep geological repository for used nuclear fuel—state of science review. In: NWMO TR-2012-02. Nuclear Waste Management Organization, Toronto, Canada.